Mon. Not. R. Astron. Soc. **387,** 1583–1588 (2008) doi:10.1111/j.1365-2966.2008.13270.x

Optimal filters for the construction of the ensemble pulsar time

Alexander E. Rodin★
Pushchino Radio Astronomical Observatory, Pushchino, Moscow region, 142290, Russia

Accepted 2008 March 31. Received 2008 March 31; in original form 2007 March 30

ABSTRACT
An algorithm of the ensemble pulsar time based on the optimal Wiener filtration method has been constructed. This algorithm allows the separation of the contributions to the post-fit pulsar timing residuals of the atomic clock and the pulsar itself. Filters were designed using the cross- and auto-covariance functions of the timing residuals. The method has been applied to the timing data of millisecond pulsars PSR B1855+09 and B1937+21 and allowed the filtering out of the atomic-scale component from the pulsar data. Direct comparison of the terrestrial time TT(BIPM06) and the ensemble pulsar time $\mathrm{PT_{ens}}$ revealed that the fractional instability of TT(BIPM06)$-\mathrm{PT_{ens}}$ is equal to $\sigma_z = (0.8 \pm 1.9) \times 10^{-15}$. Based on the σ_z statistics of TT(BIPM06)$-\mathrm{PT_{ens}}$, a new limit of the energy density of the gravitational wave background was calculated to be equal to $\Omega_{\mathrm{g}} h^2 \sim 3 \times 10^{-9}$.

Key words: methods: data analysis – pulsars: individual: PSR B1855+09 – pulsars: individual: PSR B1937+21.

1 INTRODUCTION

Following the discovery of pulsars in 1967 (Hewish et al. 1968), it became clear that their rotational stability allowed them to be used as astronomical clocks. This became even more obvious after the discovery of the millisecond pulsar PSR B1937+21 in 1982 (Backer et al. 1982). The typical accuracy of measuring the time of arrivals (TOA) of millisecond pulsar pulses is now a few microseconds, or even hundreds of nanoseconds for some pulsars. For an observation interval of the order of 10^8 s, this accuracy produces a fractional instability of 10^{-15}, which is comparable to the fractional instability of atomic clocks. Such a high stability cannot but be used for time metrology and time keeping.

There are several papers considering the applicability of the stability of pulsar rotation to time-scales. (Guinot 1988) presents the principles of the establishment of TT (terrestrial time), with the main conclusions that one cannot rely on the single atomic standard before authorized confirmation, and that, for pulsar timing, one should use the most accurate realizations of terrestrial time, e.g. TT(BIPMXX) (Bureau International des Poids et Mesures). Ilyasov et al. (1989) describes the principles of a pulsar time-scale, and the definition of a ‘pulsar second’ is presented. Guinot & Petit (1991) show that, because of the unknown pulsar period and period derivative, the rotation of millisecond pulsars is useful only for investigations of time-scale stability a posteriori and with long data spans. The papers by Ilyasov et al. (1996), Kopeikin (1997), Rodin, Kopeikin & Ilyasov (1997), and Ilyasov, Kopeikin & Rodin (1998) suggest a binary pulsar time-scale (BPT) based on the motion of a pulsar in a binary system, with theoretical expressions for variations in rotational and binary parameters depending on the observational interval. The main conclusion is that the BPT at short intervals is less stable than the conventional pulsar time-scale (PT), but, at longer periods of observation (10^2– 10^3 years), the fractional instability of BPT may be as accurate as 10^{-14}. Petit & Tavella (1996) present an algorithm of a group pulsar time-scale and some ideas concerning the stability of BPT. Finally, Foster & Backer (1990) present a polynomial approach for describing clock and ephemeris errors and the influence of gravitational waves passing through the Solar system.

In this paper, a method is presented to obtain corrections of the atomic time-scale relative to the PT from pulsar timing observations. The basic idea of the method can be found in Rodin (2006).

In Section 2, the main formulae of pulsar timing are described. Section 4 contains a theoretical algorithm for Wiener filtering. Section 5 presents the results of a numerical simulation, i.e. the recovery of the harmonic signal from noisy data by the Wiener optimal filter and the weighted average algorithms. The latter algorithm is used similarly to in Petit & Tavella (1996). Section 6 describes an application of the algorithm to the real timing data of pulsars PSR B1855+09 and B1937+21 (Kaspi, Taylor & Ryba 1994).

2 PULSAR TIMING

The algorithm for the pulsar timing is widely described in the literature (Backer & Hellings 1986; Doroshenko & Kopeikin 1990; Edwards et al. 2006). Two basic equations are presented below. The expression for the pulsar rotational phase $\phi(t)$ can be written in the

★E-mail: rodin@prao.ru

following form:

$$\phi(t) = \phi_0 + \nu t + \frac{1}{2}\dot{\nu}t^2 + \varepsilon(t), \tag{1}$$

where t is the barycentric time, ϕ_0 is the initial phase at epoch $t = 0, \nu$ and $\dot{\nu}$ are the pulsar spin frequency and its derivative, respectively, at epoch $t = 0$, and $\varepsilon(t)$ is the phase variation (timing noise). Based on equation (1), the pulsar rotational parameters ν and $\dot{\nu}$ can be determined.

The relationship between the time of arrival of a given pulse to the Solar system barycentre, t, and to the observer, $\hat{t}$, can be described by the following equation (Murray 1986):

$$c(\hat{t} - t) = -(\boldsymbol{k} \cdot \boldsymbol{b}) + \frac{1}{2R}[\boldsymbol{k} \times \boldsymbol{b}]^2 + \Delta t_{\rm rel} + \Delta t_{\rm DM}, \tag{2}$$

where $\boldsymbol{k}$ is the barycentric unit vector directed to the pulsar, $\boldsymbol{b}$ is the radius vector of the radio telescope, R is the distance to the pulsar, $\Delta t_{\rm rel}$ is the gravitational delay caused by the space–time curvature, and $\Delta t_{\rm DM}$ is the plasma delay. The pulsar coordinates, proper motion and distance are obtained from equation (2) by a fitting procedure that includes adjustment of the above-mentioned parameters to minimize the weighted sum of squared differences between $\phi(t)$ and the nearest integer.

3 FILTERING TECHNIQUE

Let us consider n uniform measurements of a random value (post-fit timing residuals) $\boldsymbol{r} = (r_1, r_2, \ldots, r_n)$. $\boldsymbol{r}$ is the sum of two uncorrelated values; that is, $\boldsymbol{r} = \boldsymbol{s} + \varepsilon$, where $\boldsymbol{s}$ is a random signal to be estimated and associated with the clock contribution, and ε is a random error associated with fluctuations in the pulsar rotation. The values $\boldsymbol{s}$ and ε should both be related to the *ideal* time-scale, as pulsars in the sky 'do not know' about the time-scales used for their timing. The problem of Wiener filtration lies in the estimation of the signal $\boldsymbol{s}$ if measurements $\boldsymbol{r}$ and covariances (3) are given (Wiener 1949; Gubanov 1997). For $\boldsymbol{r}, \boldsymbol{s}$ and ε, the covariance functions can be written as follows:

$$\begin{aligned}
&\mathrm{cov}(r, r) = \langle r_i, r_j\rangle = \langle s_i, s_j\rangle + \langle \varepsilon_i, \varepsilon_j\rangle, \\
&\mathrm{cov}(s, s) = \langle s_i, s_j\rangle, \\
&\mathrm{cov}(s, r) = \langle s_i, r_j\rangle = \langle r_i, s_j\rangle = \langle s_i, s_j\rangle, \qquad (i, j = 1, 2, \ldots, n) \\
&\mathrm{cov}(\varepsilon, \varepsilon) = \langle \varepsilon_i, \varepsilon_j\rangle,
\end{aligned} \tag{3}$$

where $\langle\rangle$ denotes the ensemble average.

The optimal Wiener estimation of the signal $\boldsymbol{s}$ and a posteriori estimation of its covariance function $\mathbf{D}_{ss}$ are expressed by the formulae (Wiener 1949; Gubanov 1997)

$$\hat{\mathbf{s}} = \mathbf{Q}_{sr}\mathbf{Q}_{rr}^{-1}\boldsymbol{r} = \mathbf{Q}_{ss}\mathbf{Q}_{rr}^{-1}\boldsymbol{r} = \mathbf{Q}_{ss}(\mathbf{Q}_{ss} + \mathbf{Q}_{\varepsilon\varepsilon})^{-1}\boldsymbol{r} \tag{4}$$

and

$$\mathbf{D}_{ss} = \mathbf{Q}_{ss} - \mathbf{Q}_{sr}\mathbf{Q}_{rr}^{-1}\mathbf{Q}_{rs}, \tag{5}$$

where the covariance matrices $\mathbf{Q}_{rr}, \mathbf{Q}_{sr}, \mathbf{Q}_{rs}, \mathbf{Q}_{ss}$ are constructed as Toeplitz matrices from the corresponding covariances. In this paper we assume that processes $\boldsymbol{s}$ and ε are stationary in a weak sense (stationary in the first and second moments). As a quadratic fit eliminates the non-stationary part of a random process (Kopeikin 1999), their covariance functions depend on the difference of the time moments $t_i - t_j$.

As it is impossible to perform pulsar timing observations without a reference clock, in order to separate the covariances, $\langle s_i, s_j\rangle$ and $\langle \varepsilon_i, \varepsilon_j\rangle$, it is necessary to observe at least two pulsars relative to the same time-scale. In this case, combining the pulsar TOA residuals and assuming that cross-covariances $\langle {}^2\varepsilon_i, {}^1\varepsilon_j\rangle = \langle {}^1\varepsilon_i, {}^2\varepsilon_j\rangle = 0$ produces (hereafter, upper-left indices run over the pulsars under consideration)

$$\langle s_i, s_j\rangle = \left(\left\langle {}^1r_i + {}^2r_i, {}^1r_j + {}^2r_j\right\rangle - \left\langle {}^1r_i - {}^2r_i, {}^1r_j - {}^2r_j\right\rangle\right) \Big/ 4, \text{ or}$$
$$\langle s_i, s_j\rangle = \left\langle {}^1r_i, {}^2r_j\right\rangle. \tag{6}$$

If M pulsars are used for the construction of the pulsar time-scale, there are $M(M-1)/2$ signal covariance estimates $\langle s_i, s_j\rangle = \langle {}^kr_i, {}^lr_j\rangle, (k, l = 1, 2, \ldots, M)$.

In equation (4), the matrix $\mathbf{Q}_{rr}^{-1}$ serves as the whitening filter. The matrix $\mathbf{Q}_{ss}$ forms the signal from the whitened data.

The ensemble signal (pulsar time-scale) is expressed as follows:

$$\hat{\mathbf{s}}_{\mathbf{ens}} = \frac{2}{M(M-1)} \sum_{m=1}^{\frac{M(M-1)}{2}} {}_m\mathbf{Q}_{ss} \cdot \sum_{i=1}^{M} {}^iw\, {}^i\mathbf{Q}_{rr}^{-1} \cdot {}^i\boldsymbol{r}, \tag{7}$$

where ${}^iw$ is the relative weight of the ith pulsar, ${}^iw = \kappa/\sigma_i^2, \sigma_i$ is the root-mean-square of the whitened data ${}^i\ \mathbf{Q}_{rr}^{-1} \cdot {}^i\boldsymbol{r}$, and κ is the constant serving to satisfy $\sum_i {}^iw = 1$. The first multiplier in equation (7) is the average cross-covariance function, and the second multiplier is the weighted sum of the whitened data.

For calculation of the auto- and cross-covariances, the following algorithm was used. The initial time-series ${}^kr_t$ were Fourier-transformed:

$${}^kx(\omega) = \frac{1}{\sqrt{n}} \sum_{t=1}^{n} {}^kr_t h_t \mathrm{e}^{i\omega t}, \quad (k = 1, 2, \ldots, M), \tag{8}$$

where the weights h_t are the zeroth-order discrete prolate spheroidal sequences (Percival 1991), which are used for optimization of broad-band bias control. They can be calculated to a very good approximation using the following formula (Percival 1991):

$$h_t = C_0' \frac{I_0\left(\pi W(n-1)\sqrt{\left[1 - \left(\frac{2t-1}{n} - 1\right)^2\right]}\right)}{I_0(\pi W(n-1))}, \tag{9}$$

where C_0' is the scaling constant used to force the convention $\sum h_t^2 = 1$, I_0 is the modified Bessel function of the first kind and zeroth order, and the parameter w affects the magnitude of the side-lobes in the spectral estimates (usually $W = 1$–4). In this paper, $W = 1$ is used.

The power spectrum $(k = l)$ and cross-spectrum $(k \neq l)$ were calculated from the formula

$${}^{kl}X(\omega) = \frac{1}{2\pi}|{}^kx(\omega){}^lx^*(\omega)|, \tag{10}$$

where $(\cdot)^*$ denotes complex conjugation.

Finally, the auto-covariance $(k = l)$ and cross-covariance $(k \neq l)$ were calculated using the following formula:

$$\mathrm{cov}({}^kr, {}^lr) = \sum_{\omega=1}^{n} {}^{kl}X(\omega)\mathrm{e}^{-i\omega t}, \quad (k, l = 1, 2, \ldots, M). \tag{11}$$

4 COMPUTER SIMULATION

To evaluate the performance of the Wiener filtering method as compared with the weighted average method, we applied it to simulated time sequences corresponding to a harmonic signal with additive white and red (correlated) noise. Simulated time-series were generated with the help of a random generator built with the MATHEMATICA software with the preset (normal) distribution for various numbers of pulsars. A maximum of 50 pulsars were used (limited by acceptable computing time). The harmonic signal to be estimated was as follows: $A\ \sin(t/P), A = 1, P = 10, t = 1, 2, \ldots, 256$. The additive Gaussian white noise had zero mean and various values of the variance. For example, in the simulation for 50 pulsars, the variance was in the range $\sigma^2 = 1, 2, \ldots, 50$. The correlated noise n_2, n_4 with the power spectra $1/f^2$ and $1/f^4$ was generated as a single or twice-repeated cumulative sum of the white noise n_0:

$$n_{2j} = \sum_{i=1}^{j} n_{0i},\ n_{4j} = \sum_{i=1}^{j} n_{2i}, \quad (j = 1, 2, \ldots, n). \tag{12}$$

The second-order polynomial trend was subtracted from the generated time-series n_2 and n_4. The weights of the individual time-series were taken to be inversely proportional to σ_z^2, where σ_z is the fractional instability (Taylor 1991). The quality of the two methods was compared by calculating the root-mean-square of the difference between the original and recovered signals.

Fig. 1 shows the results of the computer simulation described above. The quality of these two methods of signal estimation is clearly visible. It is important to note that the signal estimation accuracy in the case of the Wiener filter (solid line) is better in all cases. The most significant advantage of the Wiener filter over the weighted average method is seen in the case of the white noise (Figs 1a, b). For the correlated noise with the power spectrum $1/f^2$ (Figs 1c, d), the advantage is still clear. For the red noise with the power spectrum $1/f^4$ both methods show similar results (Figs 1e, f). Noteworthy is the dependence of the estimation quality on the observation interval for the correlated noise (Figs 1d, f): as the observation interval increases, the estimation accuracy grows. Physically, such a behaviour corresponds to the appearance of stronger and stronger variations of the correlated noise with time, which causes a deterioration in the signal estimation quality. The influences of the form of the correlated noise and length of the observation interval on the variances of the pulsar timing parameters are described in detail in Kopeikin (1997).

5 RESULTS

To evaluate the performance of the proposed Wiener filter method, timing data of pulsars PSR B1855+09 and B1937+21 (Kaspi et al. 1994) were used. For the sake of simplicity in the subsequent matrix computations, unevenly spaced data were transformed into uniformly spaced data with a sampling interval of 10 d by means of linear interpolation. Such a procedure perturbs the high-frequency component of the data while leaving the low-frequency component,

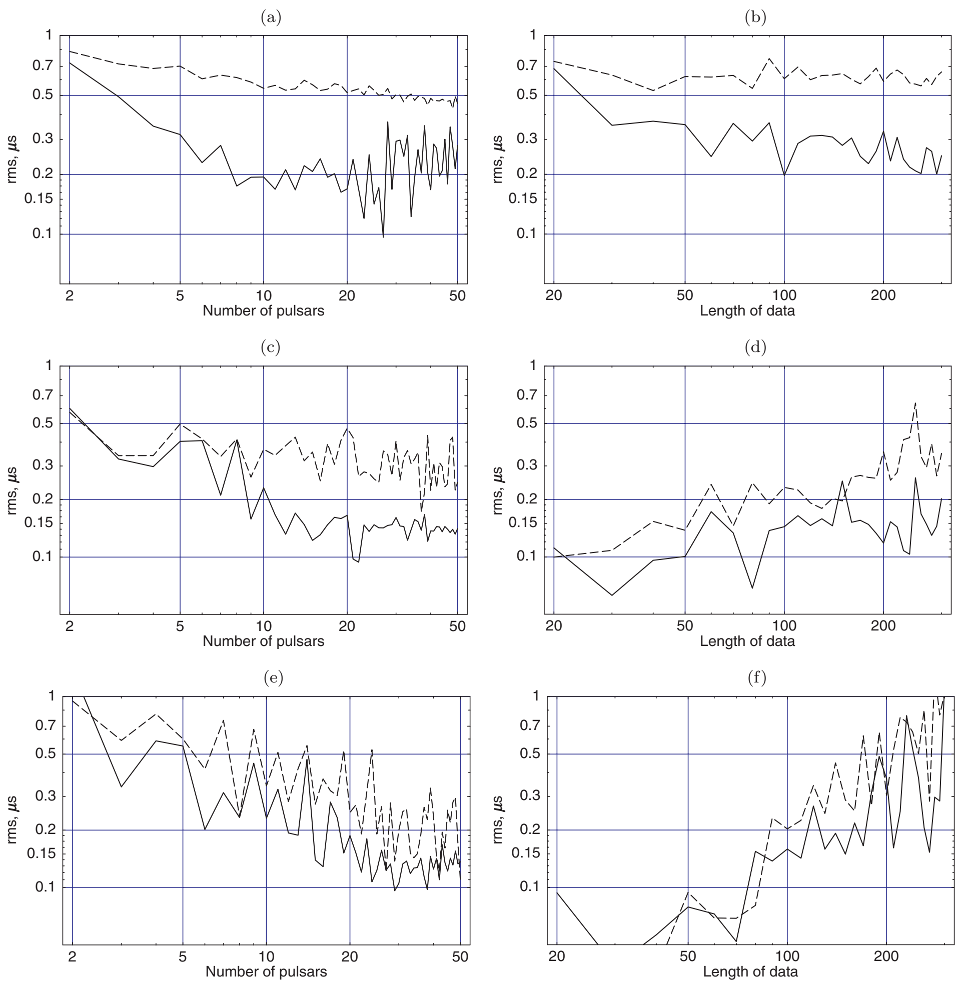

Figure 1. The accuracy of signal estimation based on the methods of weighted averages (dashed lines) and Wiener filtering (solid lines) as dependent on the number of pulsars (left panels) and length of the data (right panels). For the calculations shown in the left panels, 256 data points were taken; for the calculations shown in the right panels, five pulsars were used. Various types of noise were generated: (a), (b) white phase noise; (c), (d) white noise in frequency; (e), (f) random-walk noise in frequency. Data in the panels (d) and (f) were scaled for easy comparison with the data in the other panels.

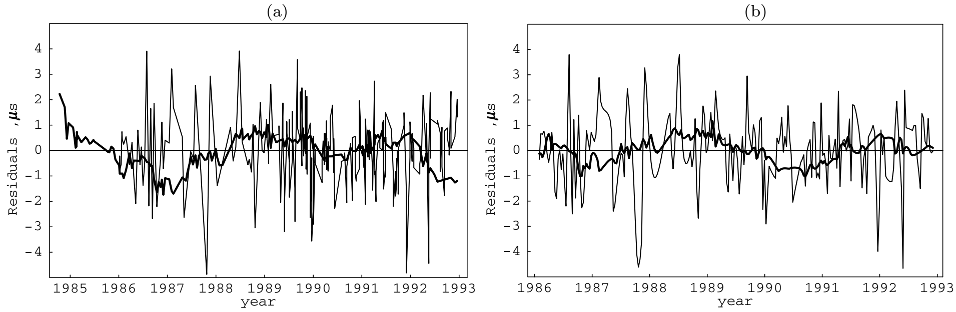

Figure 2. The barycentric timing residuals of pulsars PSR B1855+09 (thin line) and B1937+21 (thick line) (a) before and (b) after uniform sampling.

of most interest to us, unchanged. The sampling interval of 10 d was chosen to preserve approximately the same volume of data.

The common part of the residuals for both pulsars (251 TOAs) has been taken within the interval MJD = 46450–48950. As choosing the common time interval of the time-series changes the mean and slope, the residuals were quadratically refitted for consistency with the classical timing fit. The pulsar post-fit timing residuals before and after the processing described above are shown in Fig. 2.

According to Kaspi et al. (1994), the timing data of PSR B1855+09 and B1937+21 are in the UTC (Universal Coordinated Time) time-scale. UTC is the international atomic time-scale that serves as the basis for timekeeping for most of the world. UTC runs at the same frequency as TAI (International Atomic Time). It differs from TAI by an integral number of seconds. This difference increases when so-called leap seconds occur. The purpose of adding leap seconds is to keep atomic time (UTC) within ± 0.9 s of a time-scale called UT1, which is based on the rotational rate of the Earth. Local realizations of UTC exist at national time laboratories. These laboratories participate in the calculation of the international time-scales by sending their clock data to the BIPM. The difference between the UTC (computed by BIPM) and any other timing centre's UTC only becomes known after computation and dissemination of UTC, which occurs about two weeks later. This difference is presently limited mainly by the long-term frequency instability of UTC (Audoin & Guinot 2001).

The signal we need to estimate is the difference UTC−PT. Fig. 3 shows the signal estimates (thin line) based on the timing residuals of pulsars PSR B1855+09 and B1937+21 and calculated using equation (4). The combined signal (ensemble pulsar time-scale, equation 7) is shown in Fig. 4, and displays a behaviour similar to the difference UTC−TT(BIPM06) (correlation $\rho = 0.75$).

All three signals UTC−PT_{1855}, UTC−PT_{1937} and UTC−$\mathrm{PT}_{\mathrm{ens}}$ were smoothed using the following method: to decrease the Gibbs phenomenon (signal oscillations) near the ends of the smoothing interval, the series under consideration were backward and forward forecasted by p = IntegerPart $[n/2]$ lags ($n = 251$ is the length of the time-series) using Burg's (also referred to as the maximum entropy method) autoregression algorithm of order p (Burg 1975; Terebizh 1992). New time-series of double length were smoothed by use of the low-pass Kaiser filter (Gold & Rader 1973; Kaiser 1974) with a bandwidth of $f_{\max}/32$, where $f_{\max} = 2/\Delta t$, and $\Delta t = 10$ d is the sampling interval. The choice of the bandwidth was defined by visual comparison with the UTC−TT(BIPM06) line. The final time-series were obtained by dropping the forward and backward forecasted sections of the smoothed series.

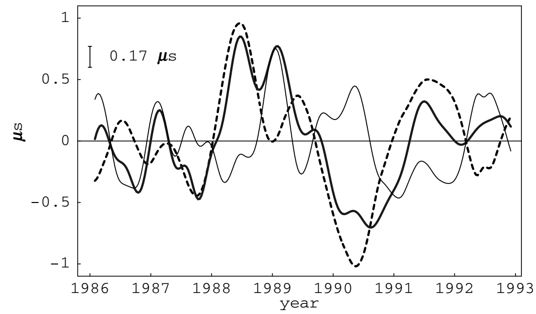

Figure 4. Combined clock variations of UTC−$\mathrm{PT}_{\mathrm{ens}}$ for the interval MJD = 46450–48950 estimated using the optimal filtering method from the timing residuals of pulsars PSR B1855+09 and B1937+21 (thick line) and the difference UTC−TT(BIPM06) (dashed line). The thin line indicates the difference TT−$\mathrm{PT}_{\mathrm{ens}}$.

The accuracy of the obtained realizations of the pulsar time-scales UTC−PT_{1855} and UTC−PT_{1937} was derived from the diagonal elements of the covariance matrix defined by equation (5). The root-mean-square values of UTC−PT_{1855} and UTC−PT_{1937} are

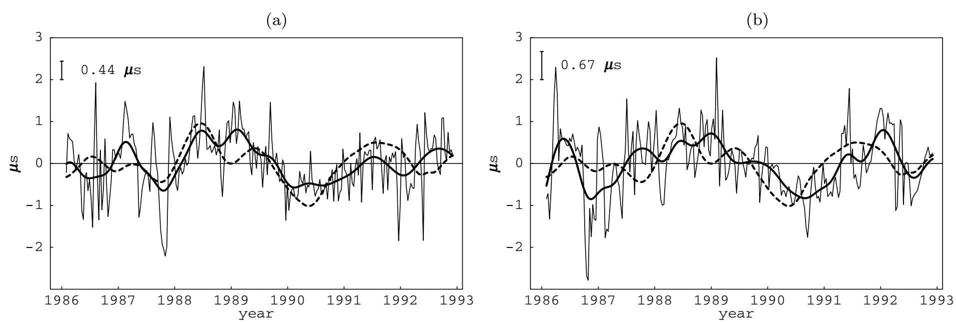

Figure 3. Differences (a) UTC−PT_{1855} and (b) UTC−PT_{1937} (thin lines) for the interval MJD = 46450–48950 estimated using the optimal filtering method of equation (4). The smoothing with the Kaiser filter is shown by the thick line. The dashed line shows the difference UTC−TT(BIPM06).

0.44 μs and 0.67 μs, respectively. The accuracy of the smoothed signals was estimated as $0.44/\sqrt{16} = 0.11$ μs and $0.67/\sqrt{16} = 0.17$ μs. Finally, for the overall accuracy a conservative estimate of 0.17 μs was derived.

6 DISCUSSION

The stability of a time-scale is characterized by the so-called Allan variance, numerically expressed as a second-order difference of the clock phase variations. As timing analysis usually includes determination of the pulsar spin parameters up to at least the first derivative of the rotational frequency, it is equivalent to excluding the second-order derivative from pulsar TOA residuals, and therefore there is no sense in the Allan variance. For this reason, for calculation of the fractional instability of a pulsar as a clock, another statistic, σ_z, has been proposed (Taylor 1991). A detailed numerical algorithm for the calculation of σ_z is described in Matsakis, Taylor & Eubanks (1997).

In this work, it has been proved that different realizations of pulsar time-scales must have comparable stabilities (Lyne & Graham-Smith 1998) and should not be worse than available terrestrial time-scales over the same interval. For this purpose, the statistic σ_z of two realizations of PT, UTC$-$PT$_{1855}$ and UTC$-$PT$_{1937}$, were compared.

Fig. 5 presents the fractional instability of the differences PT$_{1937}$ $-$PT$_{1855}$ (dashed line) and TT$-$PT$_{\mathrm{ens}}$ (solid line). For a 7-yr time interval, $\sigma_z = (0.8 \pm 1.9) \times 10^{-15}$ and $\sigma_z = (1.6 \pm 2.9) \times 10^{-15}$ for TT$-$PT$_{\mathrm{ens}}$ and PT$_{1937}$ $-$ PT$_{1855}$, respectively. It can be seen that the instability of the two differences lies within error bar intervals. The fractional instability of TT relative to PT$_{\mathrm{ens}}$ and of PT$_{1937}$ relative to PT$_{1855}$ is almost one order of magnitude better than the individual fractional instabilities of the pulsars PSR B1855+09 and B1937+21.

As an example of an astrophysical application of the fractional instability values obtained in this work, one could consider the estimation of the upper limit of the energy density of the stochastic gravitational wave background (Kaspi et al. 1994). For this purpose, theoretical lines of σ_z in the case when the gravitational wave background with the fractional energy density $\Omega_{\mathrm{g}}h^2 = 10^{-9}$ and 10^{-10} begins to dominate are plotted in the lower right-hand corner of Fig. 5. It can be seen that σ_z of TT$-$PT$_{\mathrm{ens}}$ crosses the line $\Omega_{\mathrm{g}}\ h^2 = 10^{-9}$ and approaches $\Omega_{\mathrm{g}}h^2 = 10^{-10}$. The upper limit of $\Omega_{\mathrm{g}}h^2$ based on the two-sigma uncertainty (95 per cent confidence level) of the ensemble σ_z is equal to $\sim 3 \times 10^{-9}$.

It is noteworthy that, as PSR 1855+09 and 1937+21 are relatively close to each other on the sky (angular separation of 15°.5), and hence their variations of the rotational phase contain a correlated contribution caused by the stochastic gravitational wave background (Hellings & Downs 1983), they form a good pair for estimation of the upper limit of $\Omega_{\mathrm{g}}h^2$.

Currently, the accuracy of the filtering method without the contribution of the uncertainty of the TT algorithm is estimated at a level of 0.17 μs. So, the uncertainty in PT$_{\mathrm{ens}}$ could, in principle, reach the level of a few tens of nanoseconds if it were to be used for all high-stable millisecond pulsars. As computer simulations show, for the highest advantage while applying the Wiener optimal filters one should use pulsars that show no correlated noise in their post-fit timing residuals.

7 CONCLUSIONS

An algorithm to form an ensemble pulsar time-scale based on the method of optimal Wiener filtering is presented. The basic idea of the algorithm is to use an optimal filter to remove additive noise

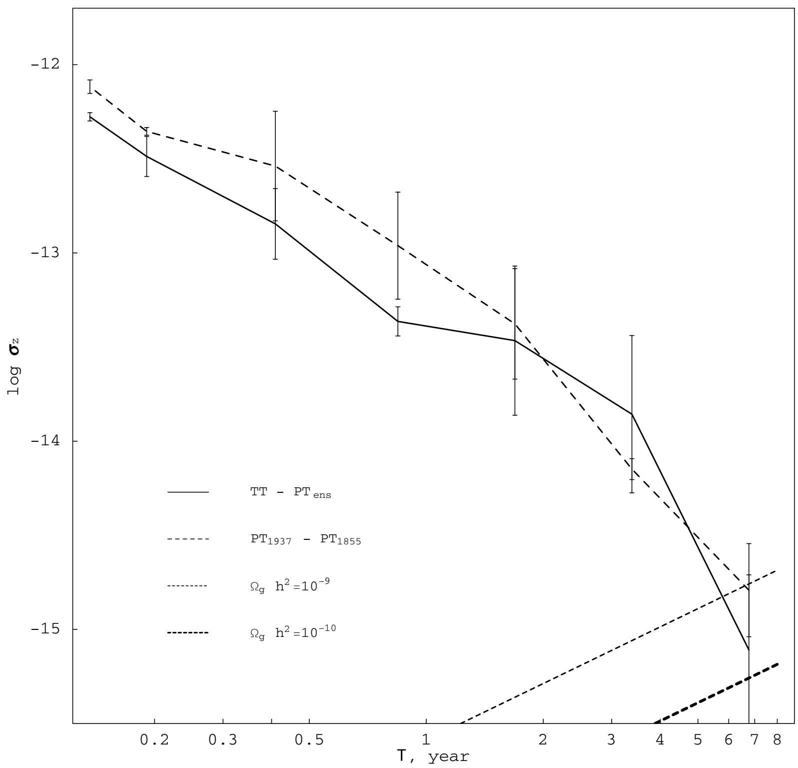

Figure 5. The fractional instability σ_z based on the difference PT$_{1937}$ $-$PT$_{1855}$ (dashed line) and σ_z of the difference TT$-$PT$_{\mathrm{ens}}$ (solid line). Theoretical values of σ_z in the cases $\Omega_{\mathrm{g}}h^2 = 10^{-9}$ and 10^{-10} are shown in the lower right-hand corner of the plot.

from the timing data *before* the construction of the weighted average ensemble time-scale.

Such a filtering approach offers an advantage over the weighted average algorithm as it utilizes additional statistical information about the common signal in the form of its covariance function or power spectrum. Because timing data are always available relative to a definite time-scale, in order to separate the pulsar and clock contributions one needs to use observations from a few pulsars (minimum two) relative to the same time-scale. Such an approach allows estimation of the signal covariance function (power spectrum) by averaging all cross-covariance functions or power cross-spectra of the original data.

The availability of two scale differences UTC−TT and UTC−PT has resulted in the long-awaited possibility of comparing the ultimate terrestrial time-scale TT and the extraterrestrial ensemble pulsar time-scale PT, of comparable accuracy. The fractional instability of TT relative to PT and their high correlation demonstrate that the PT scale can be successfully used to monitor the long-term variations of TT.

ACKNOWLEDGMENTS

This work was supported in part by the Russian Foundation for Basic Research, grant RFBR-06-02-16888.

REFERENCES

Audoin C., Guinot B., 2001, The Measurement of Time, 1st edn. Cambridge University Press, Cambridge
Backer D. C., Hellings R. W., 1986, ARA&A, 24, 537
Backer D. C., Kulkarni S. R., Heiles C. E., Davis M. M., Goss W. M., 1982, Nat, 300, 615
Burg J. P., 1975, PhD thesis, Stanford Univ.
Doroshenko O. V., Kopeikin S. M., 1990, Sov. Astron., 34, 245
Edwards R. T., Hobbs G. B., Manchester R. N., 2006, MNRAS, 372, 1549
Foster R. S., Backer D. C., 1990, ApJ, 361, 300
Gold B., Rader C. M., 1973, Digital Processing of Signals. Soviet Radio, Moscow (in Russian)
Gubanov V. S., 1997, Generalized Least-Squares. Theory and Application in Astrometry. Nauka, St Petersburg (in Russian)
Guinot B., 1988, A&A, 192, 370
Guinot B., Petit G., 1991, A&A, 248, 292
Hellings R. W., Downs G. S., 1983, ApJ, 265, L39
Hewish A., Bell S. J., Pilkington J. D. H., Scott P. F., Collinset R. A., 1968, Nat, 217, 709
Ilyasov Yu. P., Kuzmin A. D., Shabanova T. V., Shitov Yu. P., 1989, FIAN proceedings, 199, 149
Ilyasov Yu., Imae M., Kopeikin S., Rodin A., Fukushima T., 1996, in Finkelstein A. ed., Proc. Modern Problems and Methods of Astrometry and Geodynamics, p. 143
Ilyasov Yu. P., Kopeikin S. M., Rodin A. E., 1998, Astron. Lett., 24, 228
Kaiser J. F., 1974, Proc. IEEE Int. Symp. Circuits and Systems, p. 20.
Kaspi V. M., Taylor J. H., Ryba M. F., 1994, ApJ, 428, 713
Kopeikin S. M., 1997, MNRAS, 288, 129
Kopeikin S. M., 1999, MNRAS, 305, 563
Lyne A. G., Graham-Smith F., 1998, Pulsar Astronomy, 2nd edn. Cambridge University Press, Cambridge
Matsakis D. N., Taylor J. H., Eubanks T. M., 1997, A&A, 326, 924
Murray C. A., 1983, Vectorial Astrometry. Adam Hilger, Bristol
Percival D., 1991, Proc. IEEE, 79, 961
Petit G., Tavella P., 1996, A&A, 308, 290
Rodin A. E., Kopeikin S. M., Ilyasov Yu. P., 1997, Acta Cosmologica, XXIII-2, 163
Rodin A. E., 2006, Chin. J. Astron. Astrophys., 6, Suppl. 2, 157
Taylor J. H., 1991, Proc. IEEE, 79, 1054
Terebizh V. Yu., 1992, Time Series Analysis in Astrophysics. Nauka, Moscow (in Russian)
Wiener N., 1949, Extrapolation, Interpolation and Smoothing of Stationary Time Series. Wiley, New York

This paper has been typeset from a TEX/LATEX file prepared by the author.